

**DEVELOPMENT OF
NATURAL RUBBER/GRAPHENE DERIVATIVES-BENTONITE
NANOCOMPOSITES**

CHUNG CHEN SENG

**A project report submitted in partial fulfilment of the
requirements for the award of the degree of
Bachelor of Engineering (Hons) Petrochemical Engineering**

**Faculty of Engineering and Green Technology
Universiti Tunku Abdul Rahman**

September 2015

DECLARATION

I hereby declare that this project report is based on my original work except for citations and quotations which have been duly acknowledged. I also declare that it has not been previously and concurrently submitted for any other degree or award at UTAR or other institutions.

Signature : _____

Name : Chung Chen Seng

ID No. : 10AGB05576

Date : _____

APPROVAL FOR SUBMISSION

I certify that this project report entitled “**DEVELOPMENT OF NATURAL RUBBER/GRAPHENE DERIVATIVES-BENTONITE NANOCOMPOSITES**” was prepared by **CHUNG CHEN SENG** has met the required standard for submission in partial fulfilment of the requirements for the award of Bachelor of Engineering (Hons) Petrochemical Engineering at Universiti Tunku Abdul Rahman.

Approved by,

Signature : _____

Supervisor : Dr. Yamuna A/P Munusamy

Date : _____

The copyright of this report belongs to the author under the terms of the copyright Act 1987 as qualified by Intellectual Property Policy of Universiti Tunku Abdul Rahman. Due acknowledgement shall always be made of the use of any material contained in, or derived from, this report.

© 2015, Chung Chen Seng. All rights reserved.

Specially dedicated to
my beloved parents, Chung Kwai Cheng and Ong Geok Leng

ACKNOWLEDGEMENTS

I would like to thank everyone who had contributed to the successful completion of this project. I would like to express my gratitude to my research supervisor, Dr. Yamuna Munusamy for her invaluable advice, guidance and her enormous patience throughout the development of the research. My sincere thanks also goes to Dr. Mathialagan Muniyadi and Prof. Hanafi Ismail for all the support and advices.

Besides, I would like to acknowledge the support provided by Platinum Senawang Sdn. Bhd. and Universiti Sains Malaysia. In addition, I would also like to express my gratitude to my loving parent and friends who had helped and given me encouragement during the research.

**DEVELOPMENT OF
NATURAL RUBBER/GRAPHENE DERIVATIVES-BENTONITE
NANOCOMPOSITES**

Abstract

In recent years, graphene-based nanofillers have gathered attention worldwide academically and industrially. It has been proposed as a promising new material due to its outstanding physical properties such as high electron mobility, thermal conductivity, mechanical stiffness, strength and elasticity. This study was conducted to use graphene-based derivatives, graphite oxide (GO) and reduced graphite oxide (rGO) as nanofiller in natural rubber (NR) and at the same time using Bentonite (BT) clay as the dispersing agent to produce Natural Rubber/Graphene-based derivatives-Bentonite nanocomposites. This research is to look into the development of right formulation for graphene-based nanocomposites and to study which is giving optimum properties. Morphology study of the nanocomposites shows that only NR/rGO nanocomposite is having good dispersion in rubber matrix. Agglomeration occurs when BT is incorporated as shown by field emission scanning electron images for NR/GO-BT and NR/rGO-BT nanocomposites. Mechanical properties study shows that only NR/rGO nanocomposite is having improved properties with tensile strength of 18.46 MPa, modulus at 100% elongation of 6.63 MPa, modulus at 300% elongation of 7.73MPa. However, NR/rGO composite shows the lowest elongation at break of 501.60%. The highest hardness value for NR/rGO is 46.7 HRA. Oil resistance study reveals that NR/rGO nanocomposite is having the highest oil resistance with Mol% uptake of 1.24 and 1.03 for toluene and n-hexane respectively. The Swelling Index are 1.15 and 0.88 for toluene and n-hexane respectively.

TABLE OF CONTENTS

DECLARATION	i
APPROVAL FOR SUBMISSION	ii
ACKNOWLEDGEMENTS	v
ABSTRACT	vi
TABLE OF CONTENTS	vii
LIST OF TABLES	x
LIST OF FIGURES	xi
LIST OF SYMBOLS/ABBREVIATIONS	xiii
LIST OF EQUATIONS	xv
LIST OF APPENDICES	xvi

CHAPTER

1 INTRODUCTION	1
1.1 Background	1
1.2 Problem Statement	3
1.3 Research Objectives	4
2 LITERATURE REVIEW	5
2.1 Graphite and Its Derivatives	5
2.1.1 Graphene	5
2.1.2 Graphite Oxide (GO)	6
2.1.3 Reduced Graphite Oxide (rGO)	7
2.2 Oxidation and Reduction Process of Graphite	9
2.2.1 Oxidation of Graphite	9
2.2.2 Reduction of Graphite Oxide	9
2.3 Natural Rubber	11

2.4	Natural Rubber Composites	13
2.5	Natural Rubber Nanocomposites	14
2.6	Bentonite Clay	15
2.7	Bentonite Clay Nanocomposites	16
3	METHODOLOGY	17
3.1	Materials	17
3.2	Preparation of Graphite Oxide	18
3.3	Preparation of Reduced Graphene Oxide	21
3.4	Nanocomposites Preparation	23
3.4.1	Compounding	23
3.4.2	Curing, Vulcanization and Rheometer Test	24
3.5	Characterization of GNF, GO, rGO and Nanocomposites	24
3.5.1	FTIR	24
3.5.2	XRD	25
3.5.3	Raman Spectroscopy	25
3.5.4	FESEM	25
3.6	Performance Test	26
3.6.1	Tensile Test	26
3.6.2	Hardness Test	26
3.6.3	Swelling Test	26
4	RESULTS AND DISCUSSIONS	28
4.1	Characterization of GNF, GO and rGO	28
4.1.1	FTIR	28
4.1.2	XRD	31
4.1.3	Raman Spectroscopy	32
4.1.4	FESEM Analysis of GNF,GO and rGO	33
4.2	Curing Properties	34
4.3	Performance Test	35
4.3.1	Tensile Properties	35

4.4.2	Hardness Results	38
4.4.3	Chemical Resistance	39
4.4	FESEM Analysis of Nanocomposites	40
5	CONCLUSION AND RECOMMENDATIONS	42
5.1	Conclusion	42
5.2	Recommendation	43
	REFERENCES	44
	APPENDIX	54

LIST OF TABLES

TABLE	TITLE	PAGE
3.1	Compound Formulation	23
4.1	Absorption Frequency Regions and Respective Functional Groups	30
4.2	Curing Properties	34
4.3	Swelling Parameters	39

LIST OF FIGURES

FIGURE	TITLE	PAGE
1.1	Structure of Carbon Atom Arrangement in Graphene	2
2.1	Model of Graphene Carbon Atom Arrangement	5
2.2	Structure of Graphite Oxide	7
2.3	Structure of Natural Rubber	11
2.4	Sulfur Cross-Linking of Natural Rubber	12
2.5	Structure of Bentonite Clay	15
3.1	Experimental Set Up For Preparation of GO	18
3.2	Solution Stirred at 500 Rpm for 3 Hours at Room Temperature	19
3.3	GO Solution Left Overnight	20
3.4	Experimental Set Up for Preparation of rGO	21
3.5	Clear Solution Formed After Washed and Filtered	22
4.1	FTIR Spectra of GNF, GO and rGO	28
4.2	XRD Diffraction Data of GNF and GO	31
4.3	Raman Spectra of GNF and GO	32
4.4	FESEM Micrographs at 20,000X magnification of GNF, GO and rGO	33
4.5	Ultimate Tensile Strength of Nanocomposites	35
4.6	Modulus at 100% Elongation Comparison of Nanocomposites	36
4.7	Modulus at 300% Elongation Comparison of Nanocomposites	36
4.8	Percentage of Elongation at Break of Nanocomposites	37

4.9	Hardness of Nanocomposites	38
4.10	FESEM Micrographs at 300X magnification of NR, NR/GO, NR/GO-BT, NR/rGO and NR/rGO-BT Nanocomposites	41

LIST OF SYMBOLS/ABBREVIATIONS

°C	degree celcius
mm	millimeter
min	minute
rpm	revolution per minute
g	gram
ml	milliliter
MPa	mega pascal
HRA	rockwell hardness unit
%	percentage
BT	bentonite
C	carbon
CeO ₂	cerium oxide
CTAB	cetyl-trimethylammonium bromide
CRI	cure rate index
CVD	chemical vapor deposition
ENR	epoxidized natural rubber
EOMt	expanded organo-montmorillonite
FTIR	fourier transform infrared spectrophotometer
GNF	graphite nanofiber
GO	graphite oxide
HCl	hydrochloric acid
HNO ₃	nitric acid
H ₂ O ₂	hydrogen peroxide
H ₂ SO ₄	sulfuric acid

KBr	potassium bromide
KClO ₃	potassium chlorate
KMnO ₄	potassium permanganate
mH	maximum torque
mL	minimum torque
MMT	montmorillorite
NaClO ₃	sodium chlorate
NaNO ₃	sodium nitrate
NR	natural rubber
NR/GO	graphite oxide filled natural rubber nanocomposites
NR/rGO	reduced graphite oxide filled natural rubber nanocomposites
NR/GO-BT	graphite oxide and bentonite filled natural rubber nanocomposites
NR/rGO-BT	reduced graphite oxide and bentonite filled natural rubber nanocomposites
O	oxygen
OPA	oil palm ash
Pa	palygorskite
PPy	polypyrrole
rGO	reduced graphite oxide
SMR10	standard Malaysian rubber grade 10
t ₉₀	cure time
t _{s2}	scorch time
TEGO	thermally expanded graphite oxide
TEM	transmission electron microscopy
XRD	x-ray diffraction
ZnO	zinc oxide

LIST OF EQUATIONS

EQUATION	TITLE	PAGE
3.1	CRI Calculation Formula	24
3.2	Bragg's Equation	25
3.3	Mol% Uptake Calculation Formula	27
3.4	Swelling Index Calculation Formula	27

CHAPTER 1

INTRODUCTION

1.1 Background

Rubbers with fillers have been widely applied in various industrial fields due to their outstanding mechanical properties, thermal stability and oil resistance. One of the industries that requires huge amount of filled rubber is the tire industry. Tires are the essential part of automobile, whenever a new automobile is fabricated or old tires wear off after a distance of mileage was travelled and new tires are needed for replacement, there is a demand for it. Due to the high demand of tires, tire industry has become the major consumer of natural rubber.

The most widely used filler for rubber in tire industry is carbon black. A huge number of previous research studies have demonstrated whereby incorporating small amounts of particulate fillers such as carbon-black can introduce remarkable changes in the mechanical and physical properties of rubber (Li et al., 2012). Reinforcing with different types of fillers is essential for rubbers, as unfilled rubbers have very restricted applications due to their poor mechanical and physical properties. The incorporation of filler able to alter the mechanical properties of the rubber such as modulus, stiffness, stress softening effect, wearing and tearing resistance, hardness, tensile strength etc.

For the last two decades, polymer nanocomposites have got much attention worldwide academically and industrially. The incorporation of nanofillers such as

graphene, graphite oxide and reduced graphite oxide into polymer matrix creates materials that show improved physical, mechanical, dynamic mechanical, thermal, etc. properties.

Graphene, a monolayer of sp^2 -hybridized carbon atoms arranged in a two-dimensional lattice, has been proposed as a promising new material for recent years due to its outstanding physical properties such as high electron mobility, thermal conductivity, mechanical stiffness, strength and elasticity. Although graphene had been studied theoretically for decades, its actual existence was not proven until 2004, when Kostya Novoselov and Andrei Geim from the Manchester University managed to isolate a monolayer of graphene from graphite for the first time. In 2010 they were awarded the Nobel Prize (Choi and Lee, 2012). Figure 1.1 shows the structure of carbon atom arrangement in graphene.

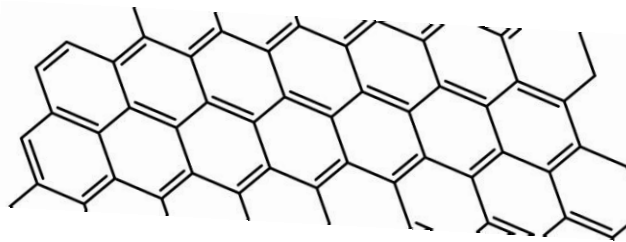


Figure 1.1: Structure of Carbon Atom Arrangement in Graphene (University of Turku, n. d.)

Graphite oxide can be produced through either Hummers or Brodie to introduce carboxyl, hydroxyl and epoxide functional groups presence at the basal planes and edges of graphite. Graphene oxide, which is a single sheet of graphite oxide atomic layer that can be produced by exfoliation of GO. The GO can be also reduced to reduced GO by chemical reduction method (Zhang et al., 2014).

In this research, we intend to use graphene-based derivatives as nanofiller in natural rubber to produce graphene-based derivatives/natural rubber nanocomposite. This research is to look into the development of right formulation for graphene-based natural

rubber nanocomposites and to study which is giving optimum properties. It is expected that this new natural rubber nanocomposite will exhibit superior strength, physical properties, and resistance to oil.

1.2 Problem Statement

Graphene is chemically inert, this prevents it from having interaction with rubber when they were mixed together. Other than that, graphene applications also being limited due to its low solubility. Moreover, since graphene is nanofiller, the amount added into the rubber will be very little. In order to achieve the enhancement of the properties of rubber, the nanofiller need to be well dispersed and homogenized with the rubber.

Therefore, in order to increase the interfacial interactions, derivatives of graphene, graphite oxide (GO) and reduced graphite oxide (rGO) were used. As both of the GO and rGO bears oxygen-containing functional groups, which enable them to disperse well in water and also in rubber. Hence, the properties of graphene are being retained. However, the reduction process can be time consuming and costly.

Moreover, we also intent to use bentonite as the dispersing agent for both the GO and rGO nanocomposites. Bentonite has a high adsorption capacity for polymers and is capable of exchanging ions on the silicate layers with reactive hydroxyl ($-OH$) groups on the surface (Ismail and Mathialagan, 2012). Thus, we propose to study the possibility of using bentonite as dispersing agent to assist dispersion of GO and rGO into the natural rubber matrix.

In this study, GO, rGO and bentonite were incorporated in natural rubber. The performance of the pure natural rubber and nanocomposites were tested and compared in terms of hardness, tensile strength, curing properties, and oil resistance. The morphology of the nanocomposites was also examined.

1.3 Research Objectives

The aims and objectives of the thesis are shown as below:

- i) To produce and characterize GO and rGO.
- ii) To produce NR/GO, NR/rGO, NR/GO-BT and NR/rGO-BT nanocomposites with two roll mill.
- iii) To study the curing characteristic, morphology, mechanical and physical properties of the nanocomposites.

CHAPTER 2

LITERATURE REVIEW

2.1 Graphite and Its Derivatives

2.1.1 Graphene

Graphene, a one-atom-thick nanosheet comprised of sp^2 hybridized carbon atoms, has exceptional mechanical properties, thermal conductivity, mobility of charge carriers and gas impermeability. (Xing et al., 2014) It has been proposed as a promising new material. A model of graphene carbon atom arrangement is illustrated in Figure 2.1

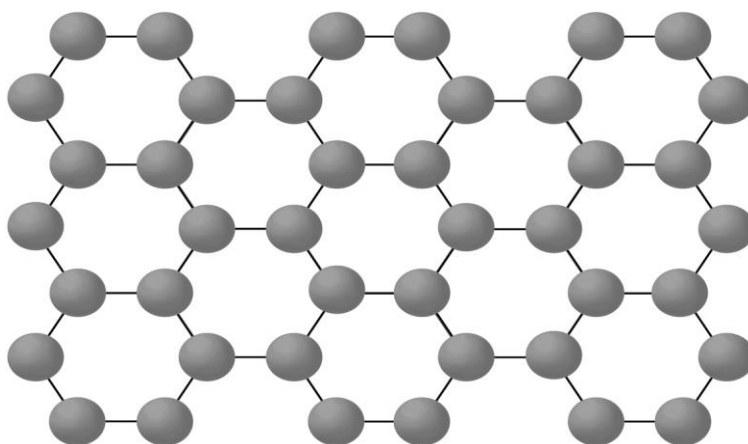


Figure 2.1: Model of Graphene Carbon Atom Arrangement (Chiappetta, M. 2015)

For the past forty years, graphene has a rich history of experimental work due to its outstanding properties that draw tremendous interest of scientists. A single, purely sp^2 -hybridized carbon layer free of heteroatomic defects, ‘Pristine’ graphene (Li et al., 2015) can be produced through several methods, including growth by chemical vapor deposition, micro-mechanical exfoliation of graphite, and growth on crystalline silicon carbide (Zhang et al., 2013). Through these methods, a largely defect-free graphene with exceptional physical properties can be produced. However, current techniques for preparing powder samples of graphene do not yield large enough quantities for use as composite filler.

Graphite oxide has been primarily utilized as the precursor material for producing graphene-based compounds. In 1960s, Boehm and coworkers reported the reduction of GO dispersion using a variety of chemical reductants such as hydrazine hydrate (Dreyer et al., 2010). Thermal expansion and thermal reduction also can produce thin, lamellar carbon containing only structure with small amounts of hydrogen and oxygen. By using transmission electron microscopy (TEM), the carbon material produced by chemical reduction was found to consist of “single carbon layers”. Liquid-phase exfoliation of graphite and chemical synthesis of graphene from polycyclic aromatic hydrocarbon precursors may also eventually provide scalable alternative routes for production of graphene, as could the further development of gas phase CVD methods (Potts et al., 2011).

2.1.2 Graphite Oxide (GO)

GO is most commonly produced by the treatment of graphite using strong mineral acids and oxidizing agents, typically via treatment with $KMnO_4$ and H_2SO_4 , as in the Hummers method or modified Hummers method, or $KClO_3$ (or $NaClO_3$) and HNO_3 as in the Staudenmaier or Brodie methods (Olanipekun et al., 2014). GO can be exfoliated using a variety of methods, most commonly by thermal shocking or chemical reduction in

appropriate media, yielding a material reported to be structurally similar to that of pristine graphene on a local scale. The chemical structure of GO is shown in Figure 2.2.

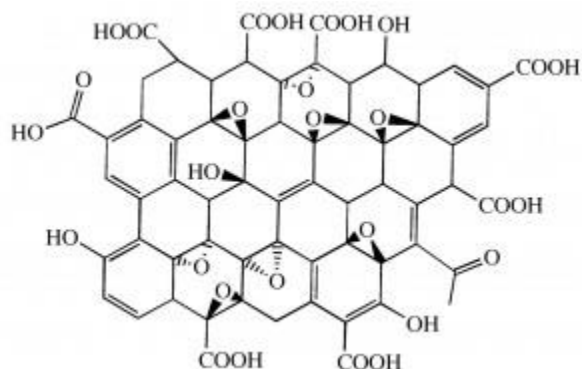


Figure 2.2: Structure of Graphite Oxide (Nationalnanomaterials, n. d.)

In terms of structure, GO contains a range of oxygen-containing functional groups such as carboxyl, hydroxyl and epoxide groups at the basal planes and edges (Lobato et al., 2014). As the oxygen-containing functional groups have high affinity to water molecules, this enables GO to disperse and form suspension in water and organic solvent. Dispersion of GO in solvent can be enhanced by inducing stirring and sonication effect (Durge, Kshirsagar and Tambe, 2014).

2.1.3 Reduced Graphite Oxide (rGO)

Reduced graphite oxide (rGO) is a material reported to be structurally similar to that of pristine graphene on a local scale. The precursor material for the production of rGO is primarily GO. rGO can be produced through several methods including thermal exfoliation, chemical vapor deposition and chemical reduction of dispersed GO. (Sun, Yu and Fugetsu, 2012) However, since reduced graphite oxide is prepared from reduction of graphite oxide, there are always some defects and some oxygen functional groups were remained in or on the reduced graphene oxide surface. Different reducing agents and methods will lead to various carbons to oxygen ratio and chemical compositions in reduced graphene oxide.

Thermal exfoliation is by applying rapid heating to GO and causes the thermal decomposition of oxygen containing functional groups in GO (Dao and Jeong, 2015). This method is fast and eco-friendly as it does not require use of any solvent or reducing agent. Moreover, due to the polar oxygen containing functional groups and the wrinkled nature, the thermally exfoliated rGO can be readily dispersed in polar organic solvent such as acetone. However, the mechanism of the interaction between thermal exfoliation and GO has not yet been carefully investigated (Wen et al., 2014).

Chemical vapor deposition (CVD) is the most appropriate growth method for producing large area and high quality single or multi layer rGO using catalytic substrates and hydrocarbons (Karamat et al., 2015). This method is most commonly applied in producing nanocomposites coated with graphitic structure such as graphitic carbon nanotubes. The formed products have high purity, allows the growth at large amount with reasonable cost and reaction occurs at moderate temperature (Atchudan et al., 2015).

Chemical reduction of GO is the most widely applied technique for preparing rGO by applying reducing agent such as hydrazine hydrate, hydroquinone, sodium borohydride and thiourea dioxide (Chua, Ambrosi and Pumera, 2012). This method allows the production of rGO at a larger quantity with low cost. However, the disadvantage of chemical reduction is that reducing agents are mostly harmful to the environment and highly toxic (Zhang et al., 2014).

2.2 Oxidation and Reduction Process of Graphite

2.2.1 Oxidation of Graphite

In year 1859, graphite oxide was first prepared by Oxford chemist, Benjamin C. Brodie. This method is by treating graphite with a mixture of potassium chlorate (KClO_3) and fuming nitric acid (HNO_3). The oxidation process was repeated for three times to ensure the oxygen composition reached the maximum (Hummers and Offeman, 1958).

After nearly 40 years later, Brodie's method has been slightly improved by L. Staudenmaier (1898) who divided the chlorate into multiple portions and added consecutively. The overall extent of oxidation achieved was similar with Brodie's approach which gives a C:O ratio of 2:1 (Gao, 2015).

In 1958, Hummers and Offeman have found out another method to synthesize GO, namely Hummers method. This method employing potassium permanganate (KMnO_4) and concentrated sulfuric acid (H_2SO_4) as oxidizing agents with the incorporation of sodium nitrate (NaNO_3). After the oxidation process, hydrogen peroxide (H_2O_2) was added into the diluted mixture in order to eliminate KMnO_4 . This method also yields the similar level of oxidation as Brodie's method. However, Hummers method requires shorter time to synthesize GO from graphite. Until today, the three methods above are still the primary routes to produce GO (Warner et al., 2013).

2.2.2 Reduction of Graphite Oxide

Reduced graphite oxide can be prepared by various methods such as chemical vapor deposition (CVD), mechanical exfoliation of graphite and reduction of graphene oxide (GO). Among these methods, the reduction of GO in organic solvents is considered

as the one of the most suitable approach due to its simplicity, reliability, suitability for large-scale production, low material cost, and versatility in chemical functionalization. (Tien et al., 2012)

The production of well-dispersed nanocomposites with GO-derived fillers is very depends on the exfoliation of GO prior to incorporation into a polymer matrix. To carry out exfoliation of GO, two techniques which are solvent-based exfoliation and thermal exfoliation techniques have emerged as two preferred routes for this step. In the former route, the hydrophilic nature and increased interlayer spacing of GO (relative to graphite) facilitates direct exfoliation into water assisted by mechanical exfoliation, such as sonication (Wallace and Moulton, 2012).

GO can also be exfoliated and reduced by rapid heating, yielding thermally expanded graphite oxide, or TEGO. In this exfoliation method, the dry powder is typically charged into a quartz tube (or other similar vessel) and subjected to thermal shock (i.e., exposure to a sudden jump in temperature), by heating to temperatures such as 400°C or higher at high rates. The rapid heating is believed to cause various small molecule species (e.g., CO, CO₂, water) to evolve and internal pressure to increase, forcing the sheets apart and yielding a dry, high-surface area material with a low bulk density (Zhao, Liu and Li, 2014).

Chemical reduction of GO manipulate the hydrophilic nature of GO. GO was directly exfoliated into water by mechanical exfoliation using ultra-sonication or stirring. Colloidal suspensions of GO platelets would be formed. Reducing agents such as hydrazine monohydrate or sodium borohydride is used to chemically reduce GO. rGO produced through this method exhibit C:O ratios of over 10:1. This reduction process can cause agglomeration of the platelets (reducing accessible surface area) unless prior steps are taken to stabilize the suspension by adjusting the pH of the suspension. (Potts et al., 2011)

2.3 Natural Rubber

Natural rubber is produced by coagulating latex by the addition of acetic or formic acid. It is a linear polymer of an unsaturated hydrocarbon called isoprene (2-methyl butadiene). Figure 2.3 shows the chemical structure of natural rubber.

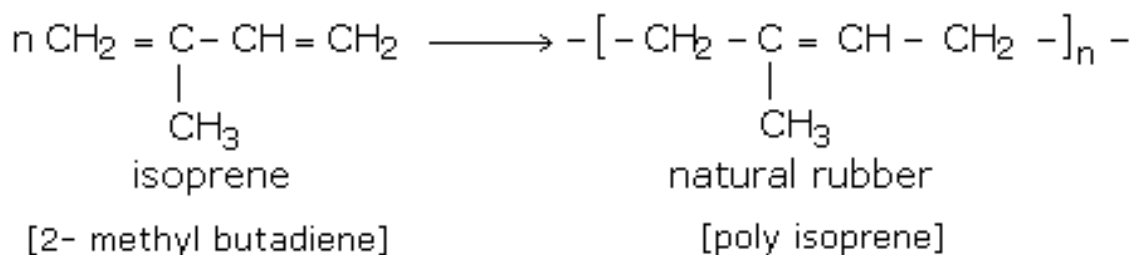


Figure 2.3: Structure of Natural Rubber (Tutorvista.com, 2015)

Crude rubber is a tough and an elastic solid. It becomes soft and sticky as the temperature rises. The most important property of natural rubber is its elasticity and flexibility. However, raw NR has low tensile strength and abrasion resistant and only has elasticity over a narrow range of temperature from 10 to 60°C. Charles Goodyear discovered the process of vulcanization in 1893 to modify the properties of natural rubber (Kohjiya and Ikeda, 2014). The sulfur cross-linking of natural rubber is shown in Figure 2.4.

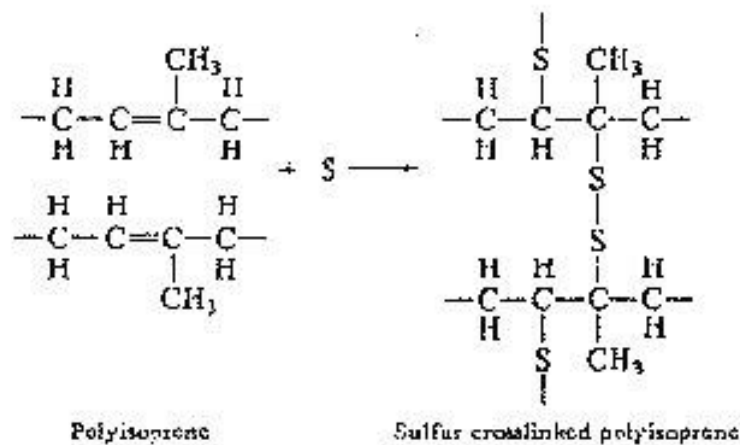


Figure 2.4: Sulfur Cross-Linking of Natural Rubber (Tutorvista.com, 2015)

Vulcanization of NR by adding a certain amount (5-8%) of sulfur forms cross-links between the molecular chains. The double bonds in natural rubber permit formation of sulfur bridges between different chains. These cross-links are responsible for removing the tackiness of untreated rubber. Vulcanized NR will have properties such as higher elasticity, tensile strength and resistance to abrasion. The improved properties of vulcanized NR allow it to have a wider application. The largest single market for vulcanized NR is automotive tires. Other products include shoe soles, bushings, seals and shock-absorbing components. Additives such as carbon black, clay, talc and calcium carbonate can be added into the NR while compounding to improve its properties as well as promote the vulcanization process (Groover, 2010).

2.4 Natural Rubber Composites

There are a number of previous studies on natural rubber composites, Xu et al., (2015) had used epoxidized natural rubber (ENR) as an interfacial modifier to improve the mechanical and dynamical mechanical properties of NR/silica composites. The NR/Silica model compound was prepared using an open mill and the interfacial interaction of ENR with silica was investigated by FTIR, TEM, X-ray diffraction (XRD) and stress-strain testing. The mechanical and dynamical mechanical properties of NR/silica composites were improved after the modification with ENR. The improvement of the properties can be attributed to the ring-opening reaction between the epoxy groups of ENR chains and Si-OH groups on the silica surface.

Other than that, Ooi, Ismail and Abu Bakar, (2014) had produced Oil Palm Ash (OPA), coated with a Liquid Epoxidized Natural Rubber (LENR) and use it as filler to be compounded with NR and other curing ingredients, using a laboratory two-roll mill. After being subjected to thermal ageing at 100°C for two days, the tensile strength and elongation at break of the LENR-coated OPA filled NR composite showed higher retention than non-coated OPA filled NR composites. Thermogravimetric Analysis (TGA) indicated that the thermal stability of LENR-coated OPA filled NR composites was higher than that of non-coated OPA filled NR composites.

Moreover, Pramila Devi et al., (2013) prepared Polypyrrole (PPy) and PPy coated short Nylon-6 fiber (F-PPy) based on NR by in situ polymerization method using anhydrous ferric chloride as oxidizing agent, *p*-toluene sulphonic acid as dopant and vulcastab VL as stabilizer. The absolute value of the dielectric permittivity, AC conductivity and absorption coefficient of the prepared conducting composites were found to be much greater than the gum vulcanizate.

2.5 Natural Rubber Nanocomposites

Nanocomposites have received considerable attention in recent years because of their diverse nanometer-sized filler particles and a series of special performance. Ortiz-Serna et al., (2014) had conducted a study on natural rubber/cellulose nanocomposites where samples with filler content from 10phr to 30phr with thickness around 0.25mm were studied under Dielectric Spectrometer. The interactions between the filler particles and the NR matrix slightly influence the electrical conductivity of the NR-cell nanocomposites. Cellulose nanoparticles maintain the inherent good dynamic properties of NR without sacrificing the insulating properties in applications where the lowest possible level of conductivity is desired.

On the other hand, Rooj et al., (2012) had prepared and studied a nanocomposite of montmorillonite clay/natural rubber with intercalation of fatty acids. Intercalation of fatty acids was done in an internal mixture, yielded expanded organo-montmorillonite (EOMt). Mixing of NR with different amounts of EOMt clay was done in an open two-roll mixing mill at 90 °C. The larger interlayer space in the presence of fatty acid promoted the exfoliation of clay minerals in NR matrix.

Another example of natural rubber nanocomposites is the palygorskite-cerium oxide filled rubber nanocomposites prepared by Zhao et al., (2012). Palygorskite (PA)-cerium oxide (CeO_2) was modified with cetyl-trimethylammonium bromide (CTAB) to be used as filler for high-performance natural rubber (NR)/styrene butadiene rubber (SBR) nanocomposites. The organic-modification of PA- CeO_2 led to good compatibility with the NR/SBR rubber matrix. The mechanical properties of the nanocomposites were significantly improved.

2.6 Bentonite Clay

Bentonite clay is one type of various inorganic filler. It is fine grained material composed of clay mineral, montmorillonite (MMT). Bentonite can be classified according to their dominant exchangeable cation. Some of the major cations are sodium, potassium, calcium, and aluminium. Bentonite has outstand others because of its unique properties which allowed it to absorb water several times of their own weight. MMT absorb water, with the basal surfaces of the clay consists of a regular arrangement of water molecules. Absorbing water will cause bentonite to form a stiff jelly and viscous substance. Figure 2.5 shows the structure of bentonite clay.

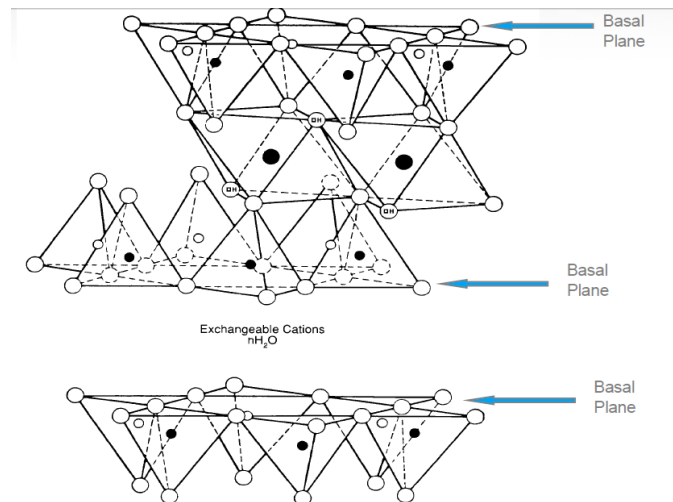


Figure 2.5: Structure of Bentonite Clay (Pixshark.com, 2015)

2.7 Bentonite Clay Nanocomposites

Clays are one of the most common fillers for polymers this is because clays are plentiful in nature and their chemical intercalation has been studied for a long time (Sanchez et al., 2009). Liborio, Oliveira and Marques, (2015) had conducted a study for the comparison of chemically modified bentonite/polypropylene nanocomposites with commercial organoclay/polypropylene nanocomposites. The results showed that nanocomposites with chemically treated bentonite clay exhibits improved degradation temperature and mechanical parameters, compared with raw polypropylene and untreated organoclay.nanocomposites.

Other than that, a study of styrene butadiene rubber (SBR)/natural rubber (NR)/bentonite (BT) nanocomposites was reported by Gu et al., (2009). The structure, mechanical properties, thermal stability and swelling behavior were examined. When the bentonite content was lower than 12 mass percent, the nanocomposites showed excellent mechanical properties. The addition of a small amount of bentonite greatly improved the thermal stability and swelling behavior, which was attributed to the good barrier properties of the dispersed and partially exfoliated organo-montmorillonite particles.

Another research study was reported by Ollier, Rodriguez and Alvarez, (2013). Unsaturated polyester/bentonite nanocomposites were prepared and characterized. The results showed that the chemical modifications of the clay caused a desired effect on its final properties improving the performance of the nanocomposites. The enhancements could be directly related to the dispersion of the clay inside the matrix.

CHAPTER 3

METHODOLOGY

3.1 Materials

In view of the conventional Hummers methods, graphene oxide (GO) was prepared from the graphite nanofiber (GNF) and other chemicals. Ultrapure deionized water (DI) was used throughout the process and can be obtained in UTAR PE lab.

The materials and reagents used were as following: Graphite nanofiber (GNF) was supplied by Platinum Senawang Sdn Bhd. Sulphuric acid (H_2SO_4 , 95%), Hydrochloric acid (HCl, 37%) and Hydrogen peroxide (H_2O_2 , 30%) were obtained from R & M Chemicals. Bentonite (BT) was supplied by Ipoh Ceramics (M) Sdn. Bhd. Sodium nitrate (NaNO_3) and Potassium permanganate (KMnO_4) were purchased from Bendosen Laboratory Chemicals. Standard Malaysian Rubber grade 10 (SMR10), zinc oxide (ZnO), stearic acid, BKF (antioxidant, 2,2'-Methylene-bis-[4-methyl-6-tert-butylphenol]), rubber vulcanization accelerator (CBS), sulphur were provided by Universiti Sains Malaysia. All chemicals were analytically pure and were used as received.

3.2 Preparation of Graphite Oxide

The conventional Hummers method was used for the synthesis of graphene oxide (GO) in this experiment (Olanipekun et al., 2014). The experimental set up for the preparation of graphene oxide was shown in Figure 3.1.

Initially, graphite nanofiber (GNF) in amount of 5.0 g was added into a 500 ml beaker loaded with 115 ml of sulphuric acid (H_2SO_4). Then, the beaker was placed under an overhead stirrer to provide homogeneous stirring at 400 rpm. An ice bath was prepared and used to maintain the temperature of beaker and reaction at 0 °C. Next, 2.5 g of sodium nitrate (NaNO_3) was added into the beaker.

After the NaNO_3 dissolved, 15.0 g of potassium permanganate (KMnO_4) was added gradually over 30 minutes to counteract overheating of the reaction mixture (<30°C). Then, a visible green suspension formed almost instantaneously.

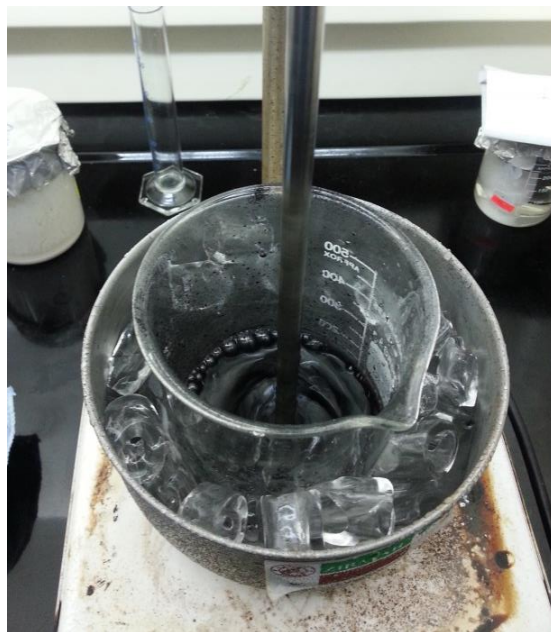


Figure 3.1: Experimental Set Up for Preparation of GO

After 10 minutes of stirring, the ice bath was removed and the temperature of the mixture was brought up to approximately 35°C. Subsequently, a purplish vapour was observed and formed as the mixture was heated up. Then, the solution was stirred vigorously at 500 rpm for duration of 3 hours at room temperature (See Figure 3.2).

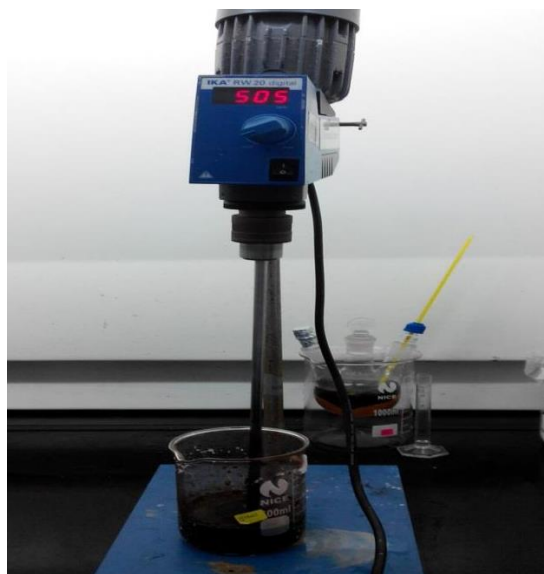


Figure 3.2: Solution Stirred at 500 Rpm for 3 Hours at Room Temperature

After 3 hours, the speed of stirrer was reduced to 400 rpm and a dark brown solution was formed. Meantime, 230 ml of ultrapure deionized water (DI) was prepared and added slowly into the solution. There was a large exothermic reaction occurred when the water was added. The temperature of the mixture increased significantly to 70°C and was maintained until the water was completely added into the solution.

The mixture was then stirred for another 10 minutes and added into 700 ml of ultrapure deionized water. Next, 12 ml of hydrogen peroxide (H₂O₂) was added in order to reduce the residual KMnO₄, resulting a light yellow suspension of graphene oxide formed. After that, the mixture was left overnight in the fume hood as shown in Figure 3.3. On the next day, the mixture showed a better colour figure where the top part showed

lighter colour and bottom part is dark. The mixture was filtered using the Whatman Anodisc membrane.



Figure 3.3: GO Solution Left Overnight.

Then, the filtered cake obtained was washed with 5 % HCl aliquots solution, followed by deionized water for several times. The washing was carried out using decantation of supernatant with centrifugation with 10,000 rpm for 20 minutes at room temperature. Finally, the pH of the supernatant was tested with pH paper and when it reached approximately in between the range of 5 to 7, the product was dispersed in deionized water and dried overnight in an oven at around 60-80°C.

3.3 Preparation of reduced graphene oxide (rGO)

The reduced graphene oxide (rGO) was prepared by chemical reduction of graphene oxide (GO) (Mitra et al., 2013). Initially, 0.08 g of GO was added into a 500 ml beaker loaded with 30 ml of ethanol. The GO suspension was then diluted with ultrapure deionized water to 250 ml. Next, the solution was sonicated for 1 hour at room temperature for well dispersed GO suspension.

After that, 100 ml of formic acid was added into the sonicated solution and the final solution was kept in a three necked round bottom flask. The solution was then stirred for 30 hours for reflux at 100 °C by using a heating mantle with magnetic stirrer. The experimental set up for the preparation of reduced graphene oxide (rGO) was shown in Figure 3.4.

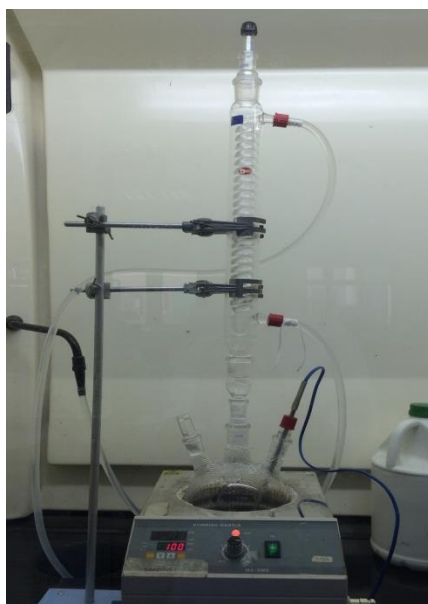


Figure 3.4: Experimental set up for preparation of reduced graphene oxide (rGO)

After 30 hours, the heating mantle was off. Then, the solution was washed and filtered with methanol, followed by ultrapure deionized water several times until a clear solution was formed (see Figure 3.5). Finally, the product was dispersed in deionized water and dried overnight in a vacuum oven at around 40-60°C to obtain reduced graphene oxide.

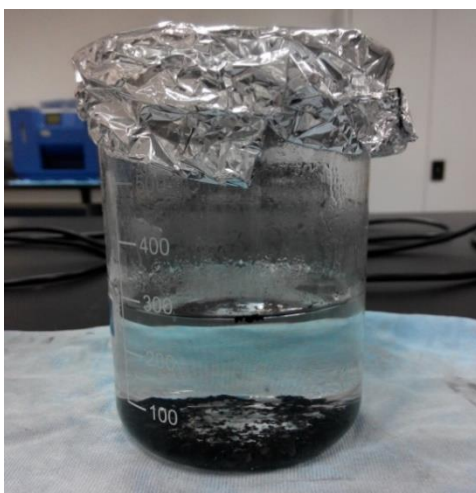


Figure 3.5: Clear solution formed after washed and filtered.

3.4 Nanocomposites Preparation

3.4.1 Compounding

Natural rubber (NR) was first masticated on the laboratory open two roll mill (XK160) for ten minutes. Zinc oxide, stearic acid and other rubber additives were added sequentially into the masticating NR. The compounds were prepared as one part of nanofiller per hundred parts of natural rubber, formulation is provided in Table 3.1 according to ASTM D3182.

Table 3.1: Compound Formulation

Ingredient	Compound (g)				
	NR	NR/GO	NR/GO-BT	NR/rGO	NR/rGO-BT
Natural Rubber	132	130.7	118.8	130.7	118.8
ZnO	6.6	6.6	6.6	6.6	6.6
Stearic Acid	4.0	4.0	4.0	4.0	4.0
BKF	1.3	1.3	1.3	1.3	1.3
CBS	2.7	2.7	2.7	2.7	2.7
Sulphur	3.4	3.4	3.4	3.4	3.4
GO	-	1.3	1.2	-	-
rGO	-	-	-	1.3	1.2
Bt	-	-	12.0	-	12.0

3.4.2 Curing, Vulcanization and Rheometer Test

The curing of samples were carried out and the curing characteristics, cure time (t_{90}), scorch time (t_{S2}), minimum torque (ML), maximum torque (MH) and cure rate index (CRI) were determined using a Monsanto Moving Die Rheometer (MDR 2000) according to ASTM D2084. Samples of respective compounds were tested at a vulcanization temperature of 150 °C. Sheets of 2 mm thickness were compressed and molded at 150 °C \pm 2 °C with 10 MPa force using a hot laboratory press at the respective cure time (t_{90}) determined with the MDR 2000.

Formula for the calculation of CRI:

$$CRI = \frac{100}{\text{cure time} - \text{scorch time}} \quad (3.1)$$

3.5 Characterization of GNF, GO, rGO and Nanocomposites

3.5.1 Fourier Transform Infrared Spectrophotometer (FTIR)

FTIR (Nicolet photospectrometer 8700) was used to provide the information regarding on the chemical bonds and molecular structure of the graphite nanofiber (GNF), graphene oxide (GO), reduced graphene oxide (rGO). Potassium bromide (KBr) pressed pellet method was applied. Analysis was conducted to determine the absorption band with a wavelength range of 4000 cm^{-1} to 400 cm^{-1} with 4 scans at a resolution of 4 cm^{-1} .

3.5.2 X-ray Diffraction (XRD)

XRD (Siemens XRD Diffractometer 5000) was used to conduct XRD analysis with specular reflection mode at room temperature. Analysis of samples were performed in the scanning range of 2θ between 0° to 80° using nickel filtered copper $K\alpha$ radiation ($\lambda=0.154\text{nm}$) at a scan rate of $1^\circ/\text{min}$. Interlayer spacing and crystalline structure of GNF and GO were recorded.

Bragg's Equation was used for the calculation of interlayer spacing :

$$d = \frac{n\lambda}{2\sin\theta} \quad (3.2)$$

where:

d = Interlayer Spacing (Armstrong)

λ = Wavelength

3.5.3 Raman Spectroscopy

The structural information of GNF and GO, were recorded using Raman Spectroscopy on NT-MDT NTEGRA with 473nm laser excitation of power 1.7mW focused through 100X objective lens to obtain the structural information of the samples. All powder samples were directly deposited on the glass slide in the absence of solvents.

3.5.4 Field Emission Scanning Electron Microscope (FESEM)

FESEM (JOEL JSM 6701F) was used to conduct analysis to determine the morphology of GNF, GO, rGO and nanocomposites. The powders were coated with thin layer of platinum before the analysis.

3.6 Performance Test

3.6.1 Tensile Test

Tensile test was carried out to determine the ultimate tensile strength, elastic modulus and percentage elongation at break of the nanocomposites. The tensile test was conducted using Tinius Olsen light weight tensile tester machine according to ASTM D412 test method using dumb-bell shaped test specimens at a uniform speed of 50mm/min.

3.6.2 Hardness Test

The hardness of the nanocomposites was measured according to ASTM D2240 test method. The average value of readings taken at five different locations on each samples at room temperature was calculated.

3.6.3 Swelling Test

Swelling behavior of the nanocomposites was measured by the change in mass of samples under the exposure of toluene and n-hexane over a period of time. Samples were immersed in toluene and n-hexane under ambient temperature for 5 days. Next, samples were removed from the liquid and quickly wiped and weighted. The samples were further dried in an oven for 24 hours at temperature of 60 °C. The dried samples were then cooled in a desiccator and weighted. The swelling parameter of respective nanocomposites were calculated and recorded.

Formulas for the calculation of swelling parameters (Ahmed et al., 2012):

a) Mol % uptake (Q_t)

$$Q_t \% = \frac{(W_1 - W_2)/W_2}{W_m} \times 100 \quad (3.3)$$

b) Swelling index (SI)

$$SI \% = (W_2 - W_1)/W_1 \times 100 \quad (3.4)$$

where:

W_1 = Initial Weight

W_2 = Swollen Wight

W_3 = Dried Weight

W_m = Molar Mass of Solvent

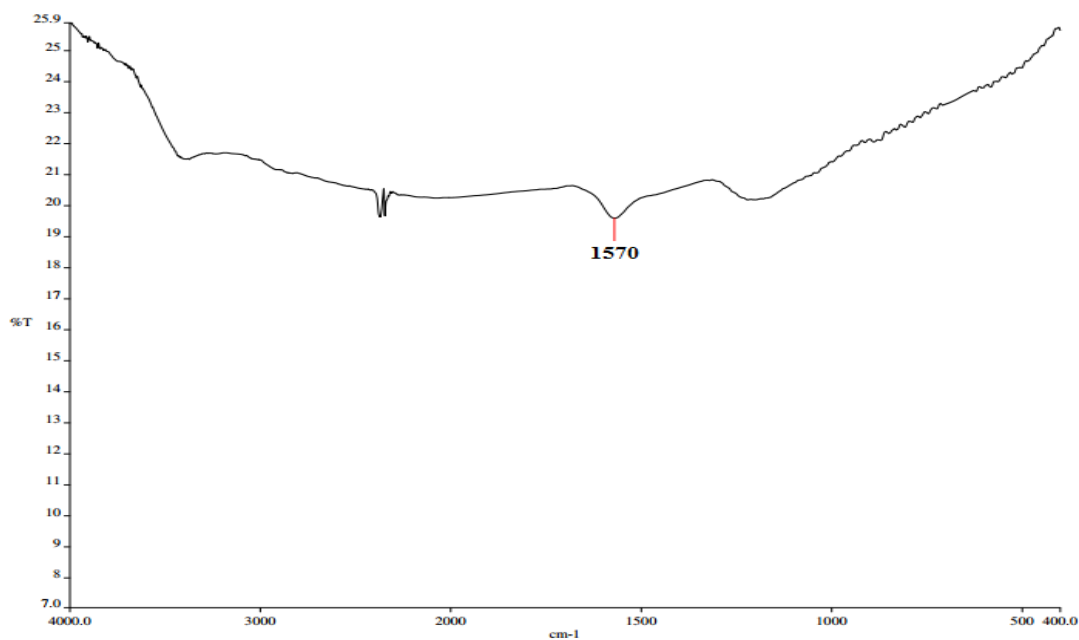
CHAPTER 4

RESULTS AND DISCUSSIONS

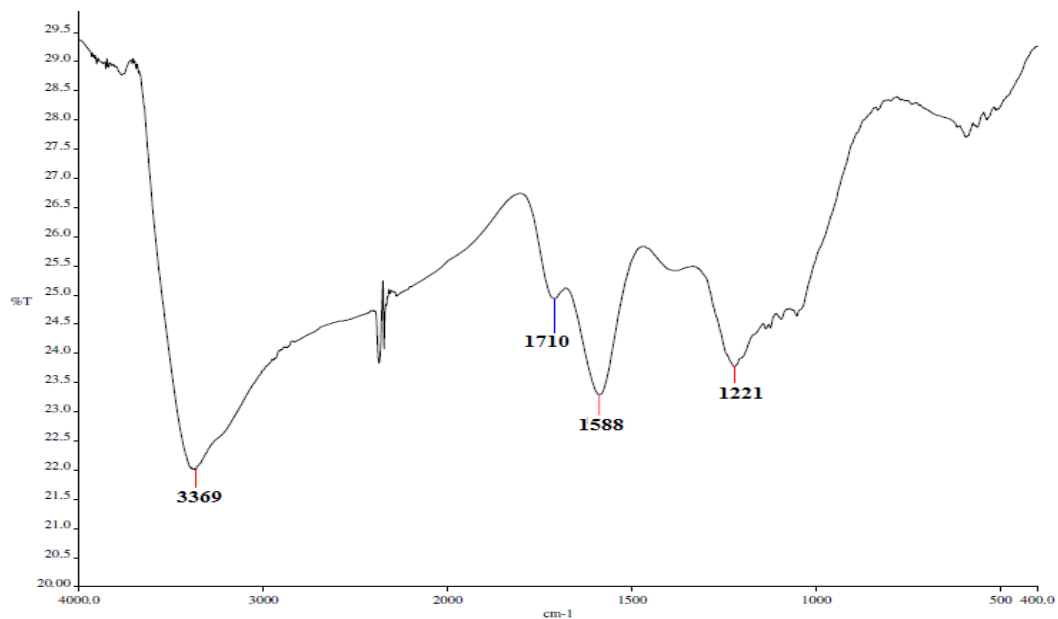
4.1 Characterization of GNF, GO and rGO

4.1.1 Fourier Transform Infrared Spectroscopy (FTIR)

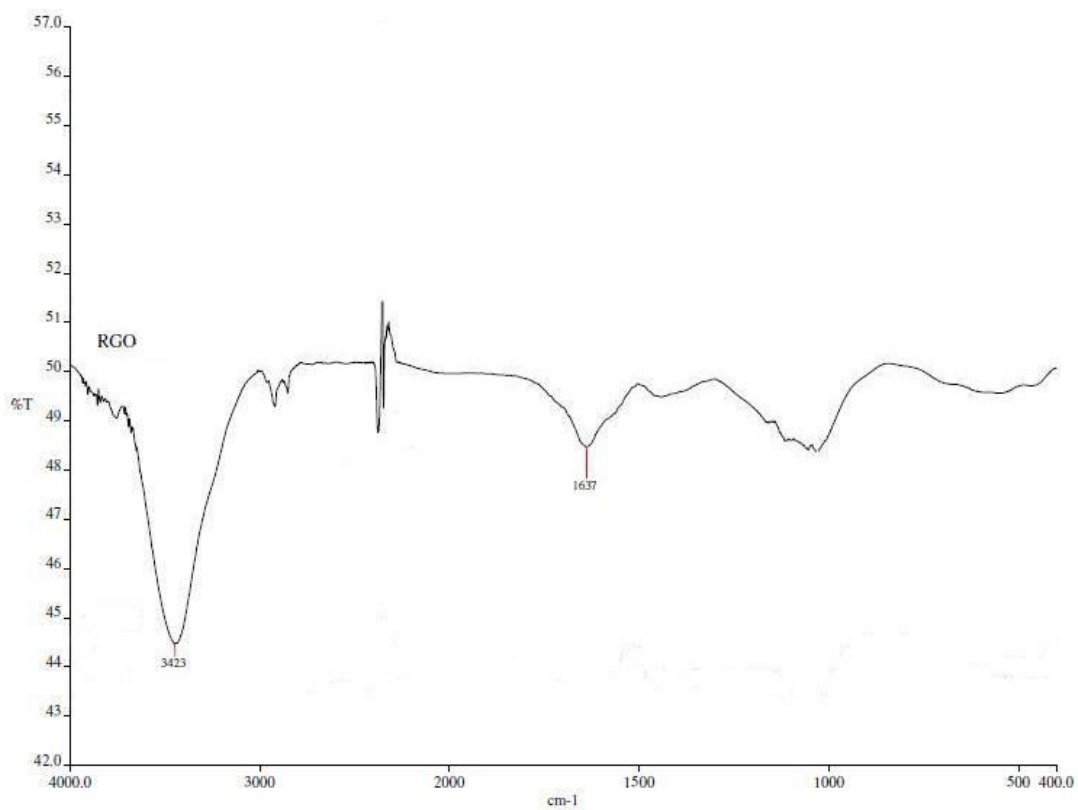
IR spectrum of GNF, GO and rGO are shown in Figure 4.1. The absorption frequency regions for the relevant functional groups are summarized in Table 4.1.



(a)



(b)



(c)

Figure 4.1: FTIR Spectra of (a) GNF, (b) GO, (c) rGO

Table 4.1: Absorption Frequency Regions and Respective Functional Groups

Absorption Frequency (cm ⁻¹)	GNF	GO	rGO	Bond	Functional Group
3550-3200		3369	3423	O-H	Alcohol/Phenol
1780-1710		1710		C=O	Carboxylic
1750-1680				C=O	Carbonyl
1700-1500	1570	1588	1637	C=C	Aromatic
1320-1210		1221		C-O	Carboxylic
1260-1000				C-O	Alcohol
1240-1040				C-O-C	Epoxide

Peak at 1570cm^{-1} in Figure 4.1(a) indicates the presence of C=C bonds for GNF. In Figure 4.1(b), a peak at 1221cm^{-1} indicates the vibration of C-O-C epoxide functional groups or C-O stretching of alcohol or carboxylic acid. Another peak at 1588cm^{-1} shows the presence of unoxidized C=C bonds in graphite oxide. The next peak at 1710cm^{-1} represents the stretching vibration of C=O bonds. At 3369cm^{-1} , the peak signifies the stretching vibration of OH groups. In Figure 4.1(c), a peak at 1570cm^{-1} was observed and this indicates the presence of C=C aromatic bond. Next, the peak at 3423cm^{-1} represents the unreduced OH bond.

The presence of oxygen-containing groups in Figure 4.1(b) has proven the oxidation of GNF to GO is successful. The removal of C=O and C-O groups at 1710cm^{-1} and 1221cm^{-1} respectively has proven the successful reduction of GO to rGO. Similar absorption peaks were reported by Olanipekun et al, (2015). Other than that, another study conducted by Tran et al, (2014) also shown similar absorption peaks for both GO and rGO.

4.1.2 X-ray Diffraction (XRD)

XRD data is shown in Figure 4.2. Diffraction peak of GNF at $2\theta = 26.3281^\circ$ associates to the spacing between the graphitic layers of 0.34nm. Whereas graphite oxide shows a relatively very low peak, indicating the preservation of unoxidized graphitic surfaces. At 12° , a peak was shown by graphite oxide with an interlayer spacing of 0.74nm. The increment of interlayer spacing is due to the presence of oxygen functionalities as it embedded into the layers. Similar peak was reported by Pendolino et al. (2015).

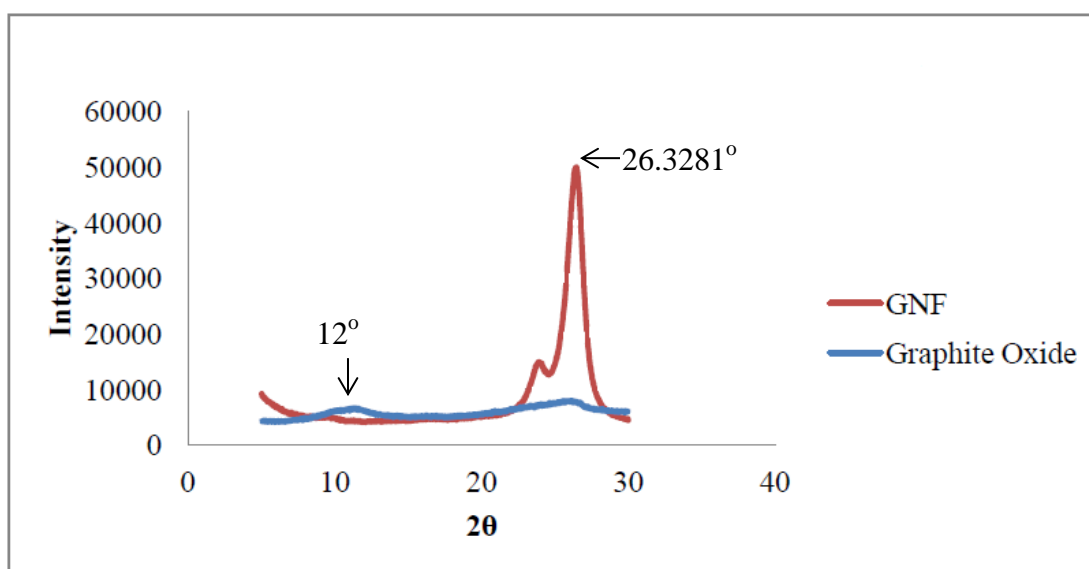


Figure 4.2: XRD Diffraction Data of GNF and GO

4.1.3 Raman Spectroscopy

The Raman spectra of GNF and GO are presented in Figure 4.3. The spectrum of GNF shows two peaks at 1587cm^{-1} (G-band) and 1349cm^{-1} (D-band). The G-band is associated to the vibration of sp^2 carbon atoms whereas D-band is attributed to the defects at the edges of the graphitic layers. On the other hand, the spectrum of graphite oxide shows a blueshift of 13cm^{-1} in the G-band, this indicates the oxidation of GNF. The intensity ratios of the D/G bands (I_D/I_G) for GNF and GO are 1.0004 and 0.9998 respectively. This proves the conversion of sp^2 carbon atoms to sp^3 carbon atoms (Hu, Song and Lopez-Valdivieso, 2015).

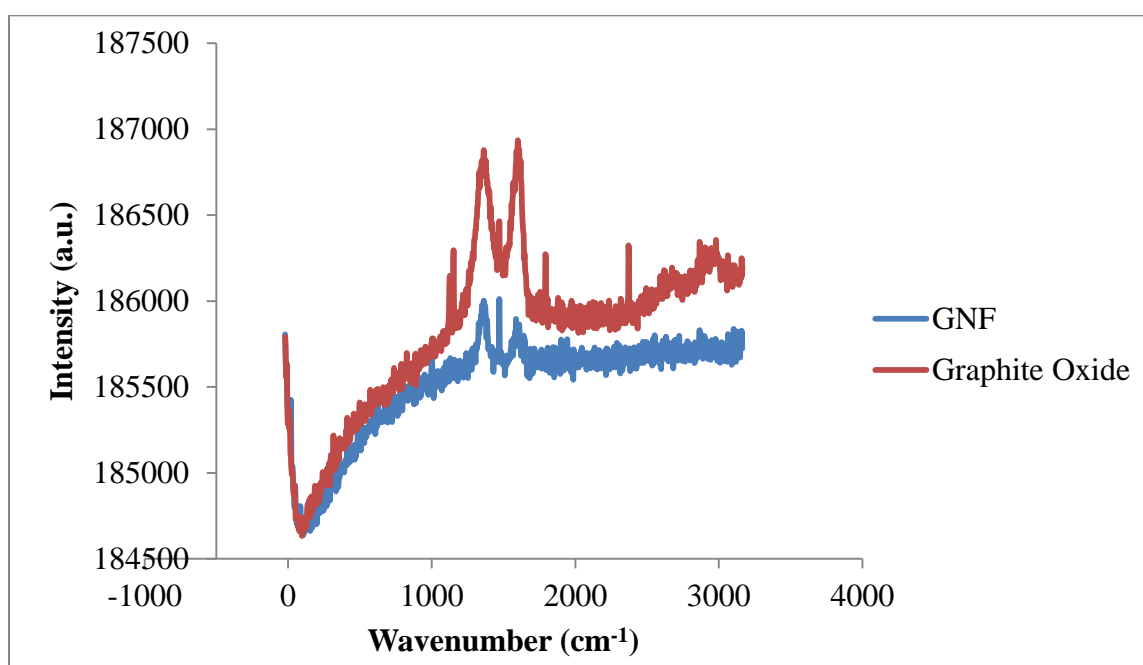
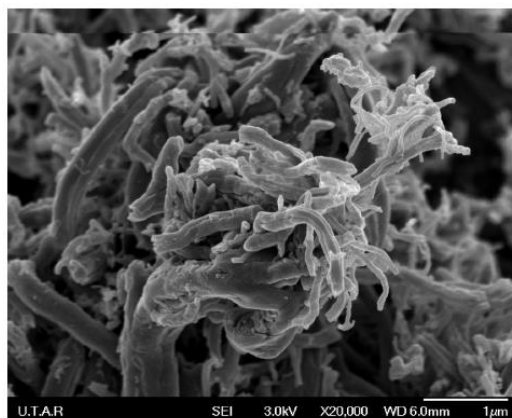


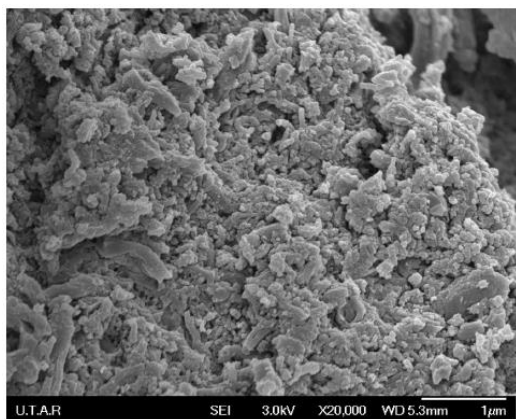
Figure 4.3: Raman Spectra of GNF and GO

4.1.4 FESEM Analysis of GNF, GO and rGO

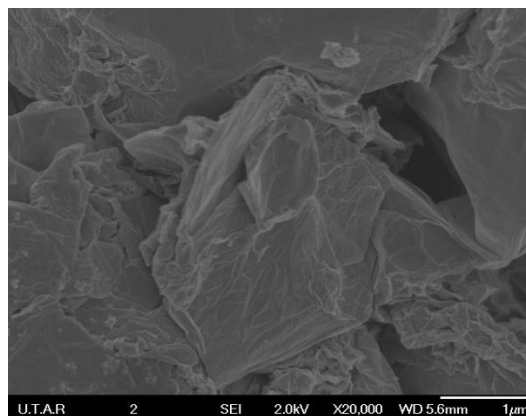
Figure 4.4 show the micrographs of GNF, GO and rGO powders under FESEM with magnification of 20,000X. From Figure 4.4(a), GNF shows coral tree-like structure. Figure 4.4(b) shows the structure of GO with a rougher surface. This is due to the presence of oxygen containing groups on the surface of graphitic layers. Similar results were reported by Zhao et al., (2014). Figure 4.4(c) shows a wrinkled paper-like structure of rGO. A study done by Silwana et al., (2015) had shown similar results.



(a)



(b)



(c)

Figure 4.4: FESEM Micrographs at 20,000X magnification of (a) GNF, (b) GO, and (c) rGO

4.2 Curing Properties

Table 4.2 shows the curing properties of the nanocomposites. The cure time (t_{90}) and scorch time (t_{S2}) for both rubber compound incorporated with bentonite (BT) are longer than the others. The longer cure and scorch time may due to the decreased thermal transition of natural rubber in presence of BT which could demote the attainment of vulcanization reaction. The cure time and scorch time of NR/rGO nanocomposites are slightly longer than control NR, yet it is still within acceptable range. The cure rate index (CRI) indicates the curing rate of samples. CRI of NR/rGO nanocomposite is very similar to that of control NR and this enables NR/rGO nanocomposite to be applied without making changes to the process parameters. Torque difference can be used as a measure of the extent of cross linking, maximum torque value and the torque difference for NR/GO and NR/rGO rubber compound are higher than those with BT, which indicates the better interaction behavior and higher interfacial adhesion between GO, rGO matrix with the NR matrix. Hence, the NR chains can be easily intercalated into the space of GO and rGO respectively as compared with the BT filled nanocomposites. Malas et al, (2012) conducted a study on expanded graphite filled natural rubber nanocomposites had proposed a similar explanation.

Table 4.2: Curing Properties

Curing Properties	Compound (g)				
	NR	NR/GO	NR/GO-BT	NR/rGO	NR/rGO-BT
ML (dNm)	0.03	0.01	0.01	0.00	0.01
MH (dNm)	7.80	7.59	6.07	6.63	5.57
Torque	7.77	7.58	6.06	6.63	5.56
Difference					
t_{90} (min)	7.50	5.99	10.04	7.83	10.16
t_{S2} (min)	2.74	2.77	4.58	3.21	4.84
CRI	21.01	31.06	18.32	21.65	18.80

4.3 Performance Test

4.3.1 Tensile Properties

Ultimate tensile strength, modulus and elongation at break of nanocomposites are recorded and shown in Figure 4.5-4.8.

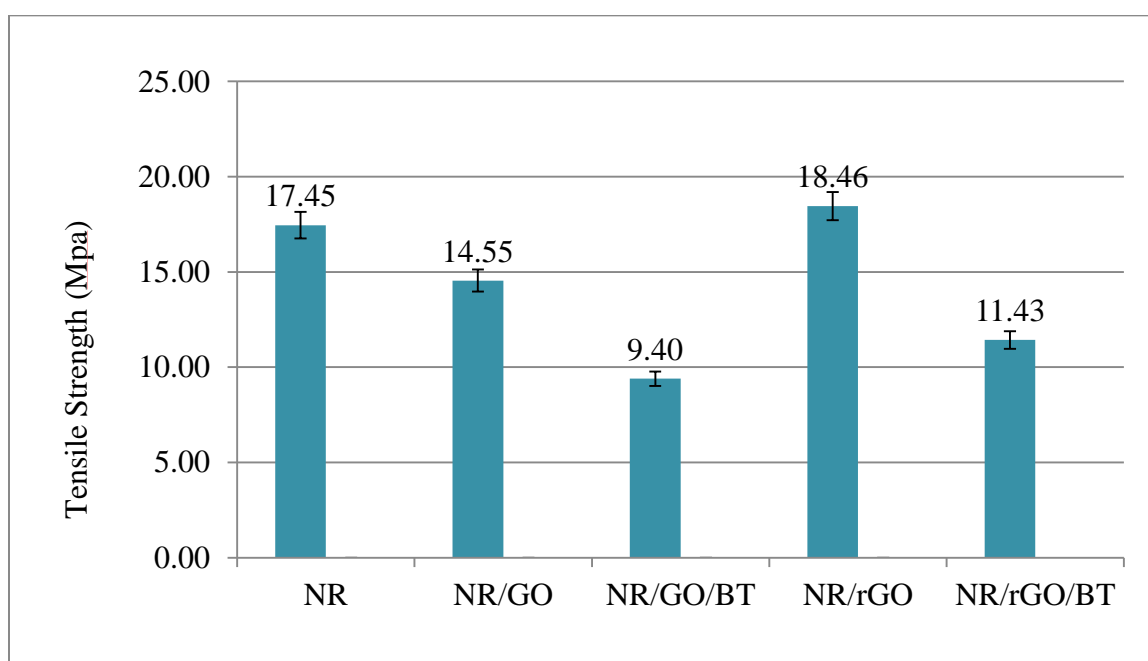


Figure 4.5: Ultimate Tensile Strength of Nanocomposites

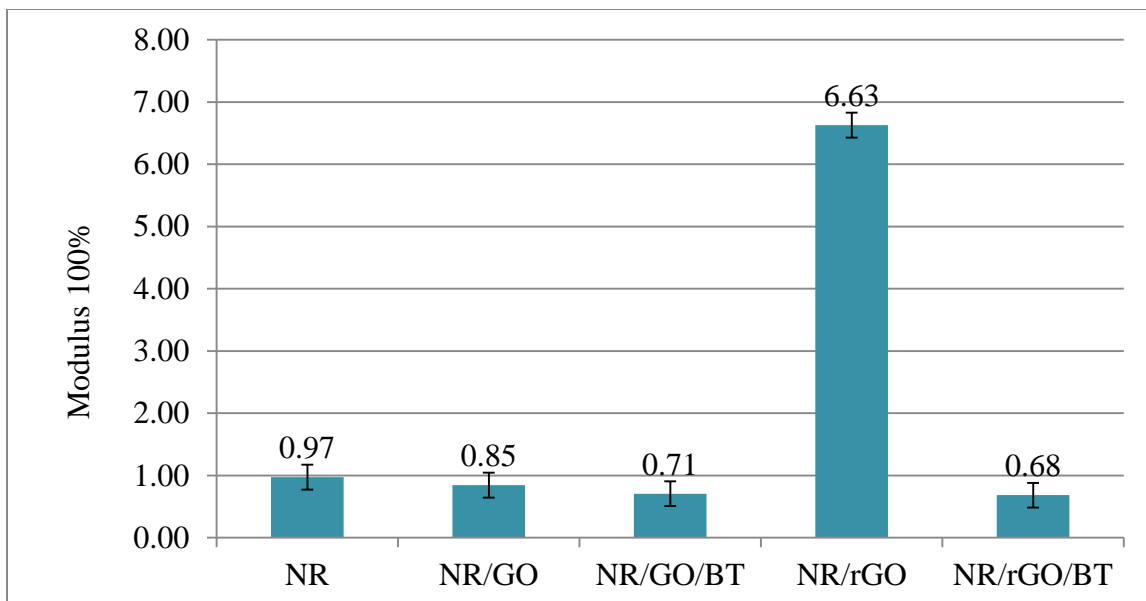


Figure 4.6: Modulus at 100% Elongation Comparison of Nanocomposites

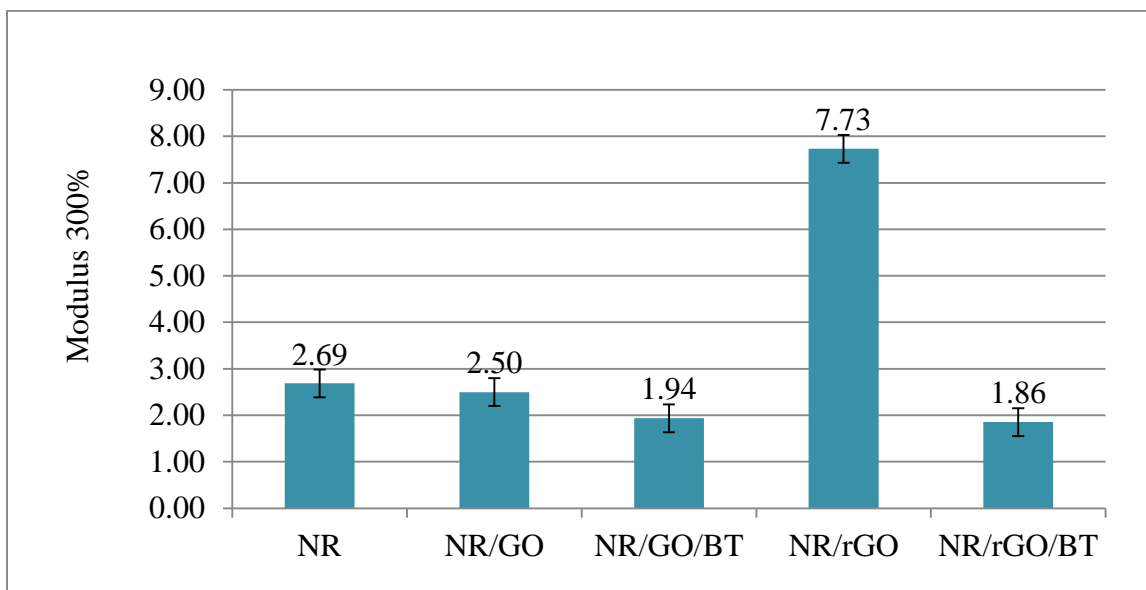


Figure 4.7: Modulus at 300% Elongation Comparison of Nanocomposites

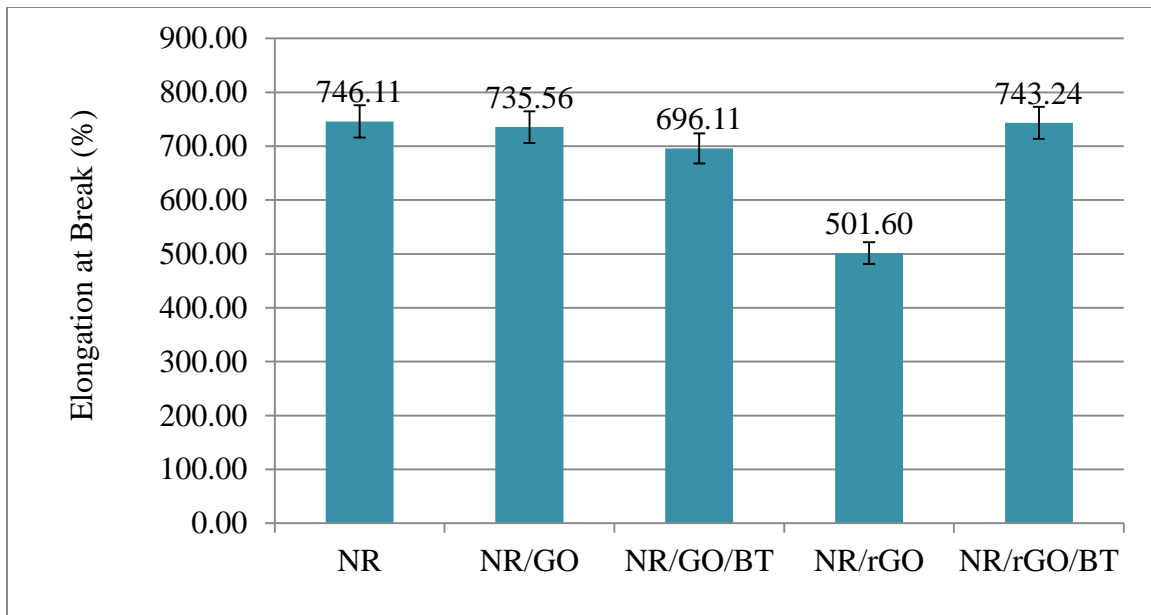


Figure 4.8: Percentage of Elongation at Break of Nanocomposites

Figure 4.5 shows that there is increase in tensile strength only in NR/rGO nanocomposites while others are lowered. Nanocomposites incorporated with BT, NR/GO-BT and NR/rGO-BT show lower tensile strength as compared to the other two NR/GO and NR/rGO nanocomposites. Figure 4.6 and Figure 4.7 show the modulus at elongation of 100% and 300% respectively. NR/rGO nanocomposites show significant increase in modulus whereas the others getting lower than the control NR. Figure 4.8 shows the percentage of elongation at break, NR/rGO nanocomposites have the lowest EB while the EB of the other three nanocomposites slightly drop.

Improvement of tensile strength in NR/rGO nanocomposite is because there is better stress transfer. rGO is able to disperse well and form better interaction with rubber matrix. On the other hand, the modulus increase and the EB of NR/rGO nanocomposite decreases. This is due to the delocalization of natural rubber chain on the surface of rGO which reduce the elasticity and increase modulus.

NR/GO-BT and NR/rGO-BT nanocomposites show a significant drop in tensile strength in Figure 4.5. As from previous study by Gu et al. (2009), BT is able to improve the mechanical properties of NR nanocomposites. However, in this research both

nanocomposites with BT show reducing mechanical properties. Hence, we propose that when GO or rGO when mix with BT, they tend to stick with each other and form agglomerates which will turn out to become stress concentration points as we observed from the micrographs through FESEM analysis in Figure 4.4(c) and Figure 4.4(e).

4.3.2 Hardness Results

Figure 4.9 show the hardness of nanocomposites. There are only slight changes in the hardness value for the nanocomposites. The hardness of NR/rGO nanocomposites is slightly increase is due to the increase of stiffness by the rGO within the NR matrix.

/

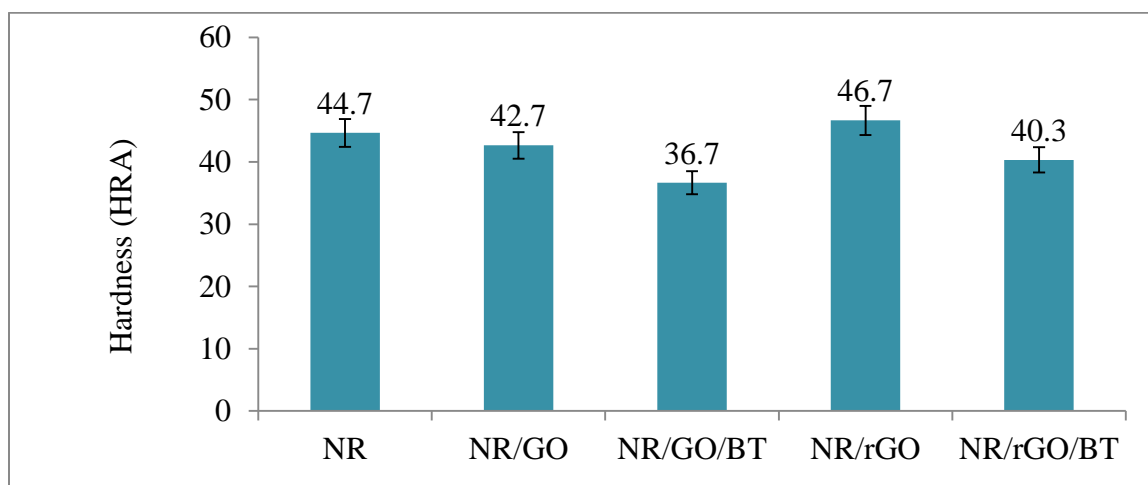


Figure 4.9: Hardness of Nanocomposites

4.3.3 Chemical Resistance

Table 4.3 illustrates the swelling parameter of nanocomposites, swelling parameters indicates the chemical resistance of the nanocomposites. It was observed that only the NR/rGO nanocomposite shows significant reduction in Mol % uptake (Q_t) and swelling index (SI). As Q_t and SI reduces, this indicates less solvent is able to penetrate into the nanocomposites. This is due to good dispersion of rGO which create tortuous path for solvent penetration. This also proves that the dispersion of rGO in the NR matrix is better. Hence, barrier layer is formed and resulting in more difficult for solvent to penetrate.

Table 4.3: Swelling Parameters

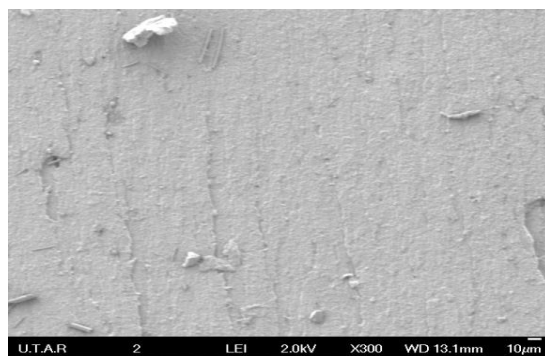
Solvent	Nanocomposites	Mol % Uptake (Q_t)	Swelling Index (SI)
Toluene	NR	1.42	1.33
	NR/GO	1.40	1.31
	NR/GO-BT	1.49	1.39
	NR/rGO	1.24	1.15
	NR/rGO-BT	1.38	1.29
n-Hexane	NR	1.13	0.99
	NR/GO	1.11	0.98
	NR/GO-BT	1.21	1.05
	NR/rGO	1.03	0.88
	NR/rGO-BT	1.09	0.95

4.4 FESEM Analysis of Nanocomposites

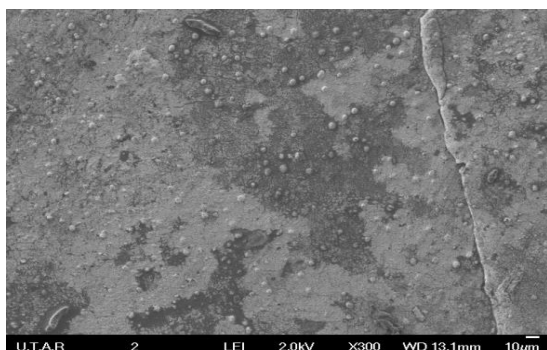
Figure 4.10 shows the micrographs of tensile fracture of pure NR, NR/GO, NR/GO-BT, NR/rGO and NR/rGO-BT nanocomposites under FESEM with magnification of 300X. From Figure 4.10(a), it was observed that the pure NR has a smooth fracture surface with no matrix tearing. The fracture is observed to propagate in major plane.

For NR/GO nanocomposite, the fracture surface is clean with no matrix tearing. Therefore still propagate in major plane as observed in Figure 4.10(b). When BT was incorporated formation of agglomerates was observed in Figure 4.10(c). The agglomeration occurred will cause the reduction of tensile strength and modulus.

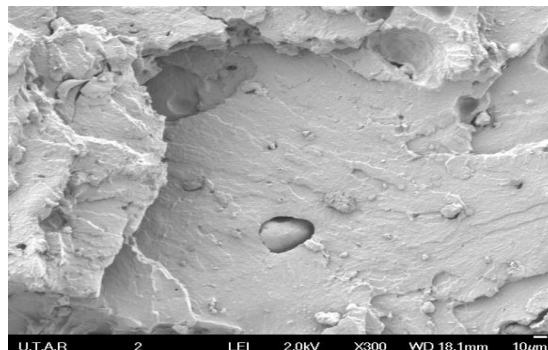
Figure 4.10(d) shows the fracture surface of NR/rGO nanocomposites with a step surface. Moreover, it was observed that there is no agglomeration at all. This indicates good dispersion of rGO in the rubber matrix and will gives better tensile properties. Figure 4.10(e) shows the fracture surface of NR/rGO-BT nanocomposites where agglomeration was observed. On the fracture surface of both NR/GO-BT and NR/rGO-BT nanocomposites, where BT is incorporated, agglomeration was observed and these agglomerates will be the stress concentration points when force is applied and lead to the reduction of tensile strength and modulus.



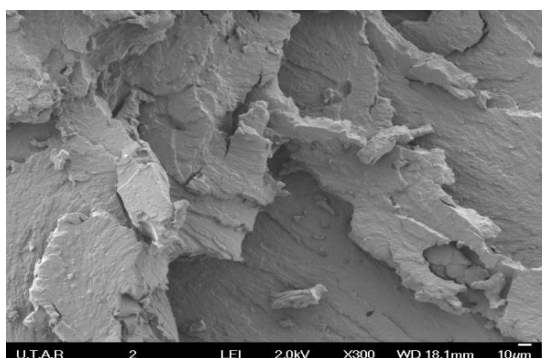
(a)



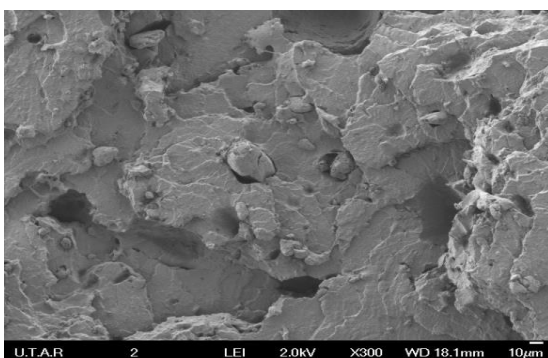
(b)



(c)



(d)



(e)

Figure 4.10: FESEM Micrographs at 300X magnification of (a) NR, (b) NR/GO, (c) NR/GO-BT, (d) NR/rGO and (e) NR/rGO-BT Nanocomposites

CHAPTER 5

CONCLUSION AND RECOMMENDATIONS

5.1 Conclusion

To conclude, GO was produced through conventional Hummers method and rGO was produced through chemically reducing GO. Characterization of GO and rGO was done via FTIR, Raman Spectroscopy and XRD. Other than that, NR/GO, NR/GO-BT, NR/rGO and NR/rGO-BT nanocomposites were successfully produced through two roll mill. The cure time and scorch time of NR/GO-BT and NR/rGO-BT nanocomposites increase significantly up to 10.04mins and 10.16mins respectively, torque difference of NR/GO-BT and NR/rGO-BT nanocomposites reduce significantly to 6.06dNm and 5.56dNm respectively while the others still within acceptable range. Morphology study of the nanocomposites shows that only NR/rGO nanocomposite is having good dispersion in rubber matrix. Agglomeration occurs when BT is incorporated as shown by NR/GO-BT and NR/rGO-BT nanocomposites. Mechanical properties study shows that only NR/rGO nanocomposite is having improved properties with tensile strength of 18.46MPa, modulus at 100% elongation of 6.63MPa, modulus at 300% elongation of 7.73MPa. However, NR/rGO composite shows the lowest elongation at break of 501.60%. The highest hardness value is NR/rGO of 46.7HRA. Oil resistance study reveals that NR/rGO nanocomposite is having the highest oil resistance with mol% uptake of 1.24 and 1.03 for toluene and n-hexane respectively. The Swelling Index are 1.15 and 0.88 for toluene and n-hexane respectively. Based on research, it is optimum to use rGO without using

dispersing agent. The mechanical and physical properties of the nanocomposite were enhanced.

5.2 Recommendation

This study has demonstrated the enhanced mechanical and physical properties of NR/rGO nanocomposites. The potential of rGO as a promising nanofiller in natural rubber has been proven. Some steps can be done in order to optimise the process and properties of the nanocomposites.

- Increase the percentage weight of rGO in natural rubber to investigate the optimum loadings of rGO while at the same time the mechanical and physical properties were not reduced.
- Determine type of dispersing agent that can be incorporated to enhance the dispersion of rGO in natural rubber matrix.
- Determine the possibilities of incorporating surface-treated rGO in natural rubber matrix.

REFERENCES

Aghigh, A., Alizadeh, V., Wong, H., Islam, M., Amin, N. and Zaman, M. (2015). Recent advances in utilization of graphene for filtration and desalination of water: A review. *Desalination*, 365, pp.389-397.

Aguilar-Bolados, H., Brasero, J., Lopez-Manchado, M. and Yazdani-Pedram, M. (2014). High performance natural rubber/thermally reduced graphite oxide nanocomposites by latex technology. *Composites Part B: Engineering*, 67, pp.449-454.

Ahmed, K., Sirajuddin Nizami, S., Zahid Raza, N. and Shirin, K. (2012). Cure Characteristics, Mechanical and Swelling Properties of Marble Sludge Filled EPDM Modified Chloroprene Rubber Blends. *AMPC*, 02(02), pp.90-97.

Atchudan, R., Perumal, S., Edison, T., Pandurangan, A. and Lee, Y. (2015). Synthesis and characterization of graphenated carbon nanotubes on IONPs using acetylene by chemical vapor deposition method. *Physica E: Low-dimensional Systems and Nanostructures*, 74, pp.355-362.

Botas, C., Álvarez, P., Blanco, P., Granda, M., Blanco, C., Santamaría, R., Romasanta, L., Verdejo, R., López-Manchado, M. and Menéndez, R. (2013). Graphene materials with different structures prepared from the same graphite by the Hummers and Brodie methods. *Carbon*, 65, pp.156-164.

Chiappetta, M. (2015). *Graphene is the super substance that could replace silicon, plastic and glass.* [online] PCWorld. Available at: <http://www.pcworld.com/article/2147304/graphene-is-the-super-substance-that-could-replace-silicon-plastic-and-glass.html> [Accessed 22 Mar. 2015].

Choi, W. and Lee, J. (2012). *Graphene*. Boca Raton: CRC Press.

Chua, C., Ambrosi, A. and Pumera, M. (2012). Graphene oxide reduction by standard industrial reducing agent: thiourea dioxide. *Journal of Materials Chemistry*, 22(22), p.11054.

Dao, T. and Jeong, H. (2015). Graphene prepared by thermal reduction–exfoliation of graphite oxide: Effect of raw graphite particle size on the properties of graphite oxide and graphene. *Materials Research Bulletin*, 70, pp.651-657.

Dineva, C. and Atanasov, V. (2013). The technical analysis of the stock exchange and physics: Japanese candlesticks for solar activity.

Dreyer, D., Park, S., Bielawski, C. and Ruoff, R. (2010). The chemistry of graphene oxide. *Chem. Soc. Rev.*, 39(1), pp.228-240.

Durge, R., Kshirsagar, R. and Tambe, P. (2014). Effect of Sonication Energy on the Yield of Graphene Nanosheets by Liquid-phase Exfoliation of Graphite. *Procedia Engineering*, 97, pp.1457-1465.

Fuente, J. (2015). *Reduced Graphene Oxide - What Is It? How Is It Created?*. [online] Graphenea. Available at: <http://www.graphenea.com/pages/reduced-graphene-oxide#.VS7G4vmUfNE> [Accessed 27 Mar. 2015].

Gadipelli, S. and Guo, Z. (2015). Graphene-based materials: Synthesis and gas sorption, storage and separation. *Progress in Materials Science*, 69, pp.1-60.

Gao, W. (2015). *Graphene Oxide: Reduction Recipes, Spectroscopy, and Applications*. New York: Springer, pp.3, 4.

Groover, M. (2010). *Fundamentals of modern manufacturing*. Hoboken, NJ: J. Wiley & Sons, pp.177, 178.

Gu, Z., Song, G., Liu, W., Li, P., Gao, L., Li, H. and Hu, X. (2009). Preparation and properties of styrene butadiene rubber/natural rubber/organo-bentonite nanocomposites prepared from latex dispersions. *Applied Clay Science*, 46(3), pp.241-244.

Hu, Y., Song, S. and Lopez-Valdivieso, A. (2015). Effects of oxidation on the defect of reduced graphene oxides in graphene preparation. *Journal of Colloid and Interface Science*, 450, pp.68-73.

Hummers, W. and Offeman, R. (1958). Preparation of Graphitic Oxide. *J. Am. Chem. Soc.*, 80(6), pp.1339-1339.

Ismail, H. and Mathialagan, M. (2012). Comparative study on the effect of partial replacement of silica or calcium carbonate by bentonite on the properties of EPDM composites. *Polymer Testing*, 31(2), pp.199-208.

Karamat, S., Sonuşen, S., Çelik, Ü., Uysallı, Y., Özgönül, E. and Oral, A. (2015). Synthesis of few layer single crystal graphene grains on platinum by chemical vapour deposition. *Progress in Natural Science: Materials International*.

Kohjiya, S. and Ikeda, Y. (2014). *Chemistry, manufacture and applications of natural rubber*. Cambridge: Elsevier, pp.119-122.

Li, L., Zeng, Z., Zou, H. and Liang, M. (2015). Curing characteristics of an epoxy resin in the presence of functional graphite oxide with amine-rich surface. *Thermochimica Acta*, 614, pp.76-84.

Li, X., Xia, Y., Li, Z. and Xia, Y. (2012). Three-dimensional numerical simulations on the hyperelastic behavior of carbon-black particle filled rubbers under moderate finite deformation. *Computational Materials Science*, 55, pp.157-165.

Liborio, P., Oliveira, V. and Marques, M. (2015). New chemical treatment of bentonite for the preparation of polypropylene nanocomposites by melt intercalation. *Applied Clay Science*, 111, pp.44-49.

Liu, D., Yang, P., Yuan, X., Guo, J. and Liao, N. (2015). The defect location effect on thermal conductivity of graphene nanoribbons based on molecular dynamics. *Physics Letters A*, 379(9), pp.810-814.

Lobato, B., Wendelbo, R., Barranco, V. and Centeno, T. (2014). Graphite Oxide: An Interesting Candidate for Aqueous Supercapacitors. *Electrochimica Acta*, 149, pp.245-251.

Malas, A., Das, C., Das, A. and Heinrich, G. (2012). Development of expanded graphite filled natural rubber vulcanizates in presence and absence of carbon black: Mechanical, thermal and morphological properties. *Materials & Design*, 39, pp.410-417.

Mikoushkin, V., Kriukov, A., Shnitov, V., Solonitsyna, A., Fedorov, V., Dideykin, A., Sakseev, D., Vilkov, O. and Lavchiev, V. (2015). Graphite oxide Auger-electron diagnostics. *Journal of Electron Spectroscopy and Related Phenomena*, 199, pp.51-55.

Mitra, M., Chatterjee, K., Kargupta, K., Ganguly, S. and Banerjee, D. (2013). Reduction of graphene oxide through a green and metal-free approach using formic acid. *Diamond and Related Materials*, 37, pp.74-79.

Olanipekun, O., Oyefusi, A., Neelgund, G. and Oki, A. (2014). Adsorption of lead over graphite oxide. *Spectrochimica Acta Part A: Molecular and Biomolecular Spectroscopy*, 118, pp.857-860.

Olanipekun, O., Oyefusi, A., Neelgund, G. and Oki, A. (2015). Synthesis and characterization of reduced graphite oxide–polymer composites and their application in adsorption of lead. *Spectrochimica Acta Part A: Molecular and Biomolecular Spectroscopy*, 149, pp.991-996.

Ollier, R., Rodriguez, E. and Alvarez, V. (2013). Unsaturated polyester/bentonite nanocomposites: Influence of clay modification on final performance. *Composites Part A: Applied Science and Manufacturing*, 48, pp.137-143.

Ooi, Z., Ismail, H. and Abu Bakar, A. (2014). Study on the ageing characteristics of oil palm ash reinforced natural rubber composites by introducing a liquid epoxidized natural rubber coating technique. *Polymer Testing*, 37, pp.156-162.

Ortiz-Serna, P., Cars[~], M., Redondo-Foj, B. and Sanchis, M. (2014). Electrical conductivity of natural rubber–cellulose II nanocomposites. *Journal of Non-Crystalline Solids*, 405, pp.180-187.

Pendolino, F., Armata, N., Masullo, T. and Cuttitta, A. (2015). Temperature influence on the synthesis of pristine graphene oxide and graphite oxide. *Materials Chemistry and Physics*.

Pixshark.com, (2015). *Pics For > Bentonite Structure*. [online] Available at: <http://pixshark.com/bentonite-structure.htm> [Accessed 2 Apr. 2015].

Potts, J., Dreyer, D., Bielawski, C. and Ruoff, R. (2011). Graphene-based polymer nanocomposites. *Polymer*, 52(1), pp.5-25.

Pramila Devi, D., Bipinbal, P., Jabin, T. and K.N. Kutty, S. (2013). Enhanced electrical conductivity of polypyrrole/polypyrrole coated short nylon fiber/natural rubber composites prepared by in situ polymerization in latex. *Materials & Design*, 43, pp.337-347.

Promdsorn, S., Moommungmee, S., Chaiyasat, P. and Chaiyasat, A. (2013). Preparation and Characterization of Natural Rubber/Poly [Styrene-co-2-(Methacryloyloxy) Ethyl Trimethylammonium Chloride] Nanocomposites by Heterocoagulation. *Energy Procedia*, 34, pp.647-655.

Ramazani, S. and Karimi, M. (2015). Aligned poly(ϵ -caprolactone)/graphene oxide and reduced graphene oxide nanocomposite nanofibers: Morphological, mechanical and structural properties. *Materials Science and Engineering: C*, 56, pp.325-334.

Rooj, S., Das, A., StÄ¶ckelhuber, K., Mukhopadhyay, N., Bhattacharyya, A., Jehnichen, D. and Heinrich, G. (2012). Pre-intercalation of long chain fatty acid in the interlayer space of layered silicates and preparation of montmorillonite/natural rubber nanocomposites. *Applied Clay Science*, 67-68, pp.50-56.

Sanchez, S.S., Nonell, J.M., Rodriguez, F.J.M., Vargas, E.R., Colunga, H.S., Valdez, J.G.M., Jimenez, L.M., Velasquez, G.N., 2009. Effect of PEGMA/amine silane compatibilizer on clay dispersion of polyethylene–clay nanocomposites. *Polym. Bull.* 63, 921–933.

Services, N. (2015). *The Complete Technology Book On Plastic Films, Hdpe And Thermoset Plastics by Niir Board Of Consultants & Engineers*. [online] NIIR Project Consultancy Services. Available at: <http://www.niir.org/books/book/complete-technology-book-on-plastic-films-hdpe-thermoset-plastics-niir-board-consultants-engineers/isbn-8178330113/zb,,10c,a,18,0,3e8/index.html> [Accessed 28 Mar. 2015].

Silwana, B., Horst, C., Iwuoha, E. and Somerset, V. (2015). Synthesis, characterisation and electrochemical evaluation of reduced graphene oxide modified antimony nanoparticles. *Thin Solid Films*, 592, pp.124-134.

Sun, L., Yu, H. and Fugetsu, B. (2012). Graphene oxide adsorption enhanced by in situ reduction with sodium hydrosulfite to remove acridine orange from aqueous solution. *Journal of Hazardous Materials*, 203-204, pp.101-110.

Tien, H., Luan, V., Lee, T., Kong, B., Chung, J., Kim, E. and Hur, S. (2012). Enhanced solvothermal reduction of graphene oxide in a mixed solution of sulfuric acid and organic solvent. *Chemical Engineering Journal*, 211-212, pp.97-103.

Tran, M., Yang, C., Yang, S., Kim, I. and Jeong, H. (2014). Influence of graphite size on the synthesis and reduction of graphite oxides. *Current Applied Physics*, 14, pp.S74-S79.

Tutorvista.com, (2015). *Natural Rubber, Properties of Natural Rubber | Tutorvista.com*. [online] Available at: <http://www.tutorvista.com/content/chemistry/chemistry-ii/carbon-compounds/natural-rubber.php> [Accessed 27 Mar. 2015].

Wallace, G. and Moulton, S. (2012). *Organic bionics*. Weinheim: Wiley-VCH.

Warner, J., Schaffel, F., Rummeli, M. and Bachmatiuk, A. (2013). *Graphene: Fundamentals and emergent applications*. Amsterdam: Elsevier.

Wen, C., Zhao, N., Zhang, D., Wu, D., Zhang, Z. and Zhang, S. (2014). Efficient reduction and exfoliation of graphite oxide by sequential chemical reduction and microwave irradiation. *Synthetic Metals*, 194, pp.71-76.

Xia, H., Zhang, X., Shi, Z., Zhao, C., Li, Y., Wang, J. and Qiao, G. (2015). Mechanical and thermal properties of reduced graphene oxide reinforced aluminum nitride ceramic composites. *Materials Science and Engineering: A*, 639, pp.29-36.

Xing, W., Tang, M., Wu, J., Huang, G., Li, H., Lei, Z., Fu, X. and Li, H. (2014). Multifunctional properties of graphene/rubber nanocomposites fabricated by a modified latex compounding method. *Composites Science and Technology*, 99, pp.67-74.

Xu, T., Jia, Z., Luo, Y., Jia, D. and Peng, Z. (2015). Interfacial interaction between the epoxidized natural rubber and silica in natural rubber/silica composites. *Applied Surface Science*, 328, pp.306-313.

Yaragalla, S., A.P., M., Kalarikkal, N. and Thomas, S. (2015). Chemistry associated with natural rubber-graphene nanocomposites and its effect on physical and structural properties. *Industrial Crops and Products*, 74, pp.792-802.

Zhang, X., Li, K., Li, H. and Lu, J. (2013). Dipotassium hydrogen phosphate as reducing agent for the efficient reduction of graphene oxide nanosheets. *Journal of Colloid and Interface Science*, 409, pp.1-7.

Zhang, X., Li, K., Li, H., Lu, J., Fu, Q. and Chu, Y. (2014). Graphene nanosheets synthesis via chemical reduction of graphene oxide using sodium acetate trihydrate solution. *Synthetic Metals*, 193, pp.132-138.

Zhao, G., Shi, L., Feng, X., Yu, W., Zhang, D. and Fu, J. (2012). Palygorskite-cerium oxide filled rubber nanocomposites. *Applied Clay Science*, 67-68, pp.44-49.

Zhao, J., Liu, L. and Li, F. (2014). *Graphene Oxide: Physics and Applications*. New York: Springer, pp.2, 3.

Zhao, W., Kido, G., Hara, K. and Noguchi, H. (2014). Characterization of neutralized graphite oxide and its use in electric double layer capacitors. *Journal of Electroanalytical Chemistry*, 712, pp.185-193.

Zhao, Y., Wu, Z. and Bai, S. (2015). Study on thermal properties of graphene foam/graphene sheets filled polymer composites. *Composites Part A: Applied Science and Manufacturing*, 72, pp.200-206.

APPENDIX